J. Fluid Mech. (2005), *vol.* 523, *pp.* 79–98.
DOI: 10.1017/S0022112004002290 Printed in the United Kingdom

What determines the thickness of layers in a thermohaline staircase?

By TIMOUR RADKO

Department of Oceanography, Naval Postgraduate School, 833 Dyer Road, Room SP-344, Monterey, CA 93943, USA
tradko@nps.edu

(Received 27 January 2004 and in revised form 29 June 2004)

A simple theory is developed for the equilibrium height of steps in a thermohaline staircase. The model is based on a linear stability analysis for a series of salt-finger interfaces, which reveals a tendency for the staircase to evolve in time until the characteristic thickness of layers reaches a critical value (H_0). Relatively thin layers successively merge as a result of the parametric variation of the heat/salt flux ratio (γ), but these mergers cease when the thickness of layers exceeds H_0. The equilibration of thick steps in our model is caused by the slight inhomogeneity of the convecting layers which has a stabilizing effect on the staircase. The instability theory is successfully tested against fully nonlinear numerical simulations and is qualitatively consistent with oceanic observations.

1. Introduction

When the density of a fluid is determined by two components, which diffuse at different rates, the flow can become unstable even if the density of the fluid is increasing downwards. The resulting double-diffusive convection has long been recognized as a significant, and in many cases dominant, mixing process in the ocean. Under typical conditions in the subtropical oceans (hot salty fluid above the cold and fresh), the faster diffuser (T) is stabilizing and the slower diffuser (S) is destabilizing, leading to the salt-fingering instability, which is a primary focus of our study.

One of the most intriguing aspects of double-diffusive convection is related to its ability to transform smooth vertical gradients into a stepped structure consisting of mixed layers separated by thin stratified interfaces. Persistent staircases have been well documented in the Tyrrhenian Sea, below the Mediterranean outflow, and in the western tropical North Atlantic (Schmitt 1994). Spontaneous layer formation from the uniform gradients was also observed in laboratory experiments (Krishnamurti 2003).

Several hypotheses have been put forward to explain the origin of thermohaline staircases. These include the collective instability theory (Stern 1969) and a notion that the steps represent thermohaline intrusions evolving into a staircase (Merryfield 2000); see the discussion in Radko (2003, referred to as R03 hereafter). However, it was recently suggested, and confirmed by direct numerical simulations (R03), that layers form as a result of the instability of the flux gradient laws (Walsh & Ruddick 2000). Linear stability analysis shows that the uniform temperature–salinity gradient is unstable in the parameter range where the flux ratio of diffusing substances

$\gamma = \alpha F_T / \beta F_S$ decreases with the density ratio $R = \alpha T_z / \beta S_z$. This instability manifests itself in the form of growing, horizontally uniform perturbations, which eventually transform the basic gradient into a well-defined thermohaline staircase. Layers that initially develop in the numerical simulations (R03) are relatively thin and unsteady. They merge continuously, and the characteristic height of steps increases in time correspondingly.

The merger of layers can be explained by stability analysis for a series of interfaces (Huppert 1971; R03), which indicates that strong interfaces, characterized by large temperature and salinity jumps, grow further at the expense of weaker interfaces. The weak interfaces gradually erode and ultimately disappear. The merger events in the R03 model continue indefinitely, and questions related to staircase equilibration and selection of the preferred scale of layers have been left unanswered.

A principal feature of the stability analysis in R03 is the assumption that the convecting layers are homogeneous; small variations in temperature, salinity, and density in the mixed layers were neglected. However, it is the variation in density that drives the convective overturning in layers and, we argue, it should be included in a complete theory of the thermohaline staircase. While the model in R03 explains the merger of thin layers, it becomes inadequate when layers become sufficiently thick. In particular, we now demonstrate that the slight inhomogeneity of the convecting layers has a stabilizing effect on a staircase, eventually suppressing the spontaneous merger events.

The objective of this study is to develop a theory for the equilibrium height of steps in a thermohaline staircase. The paper is set out as follows. In § 2 we perform a linear stability analysis for a series of interfaces, taking the density variation in the convecting layers into account. The instability theory indicates that layers tend to merge if their characteristic thickness H is less than a critical value H_0, which is determined by the background gradients of temperature and salinity, and remain steady if H exceeds H_0. It is then suggested (§ 3) that the thickness of the observed layers corresponds to the marginal instability condition $H = H_0$. The inferences from the linear analysis are supported by the nonlinear numerical simulations in § 4. Results are summarized and related to the oceanographic observations in § 5.

2. Instability of a series of interfaces

To gain a preliminary understanding of the interaction between layers in a thermohaline staircase, we consider the dynamics of a simple, yet illuminating system in figure 1. The schematic diagram in figure 1(*a*) shows a basic state consisting of a series of identical thin salt-finger interfaces separated by convecting layers of equal thickness H. Following R03, we perturb this steady state as indicated in figure 1(*b*). We increase slightly the T, S jump at the interface $z = z_1$, but decrease the jump at the adjacent interfaces; the vertical structure is assumed to be periodic with the z-wavelength of $2H$. Thus, the state in figure 1(*b*) can be thought of as an infinite series of layers in which we simultaneously reduce the magnitude of $(\Delta T, \Delta S)$ at all steps with even numbers and correspondingly increase the T, S jumps across the odd steps. Note that such a perturbation does not affect the overall T, S gradient. Our objective is to determine whether the disturbance will grow in time, implying instability of the basic state in figure 1(*a*), or remain small. The essential difference between this model and the one studied in R03 is that the convecting layers are not necessarily homogeneous.

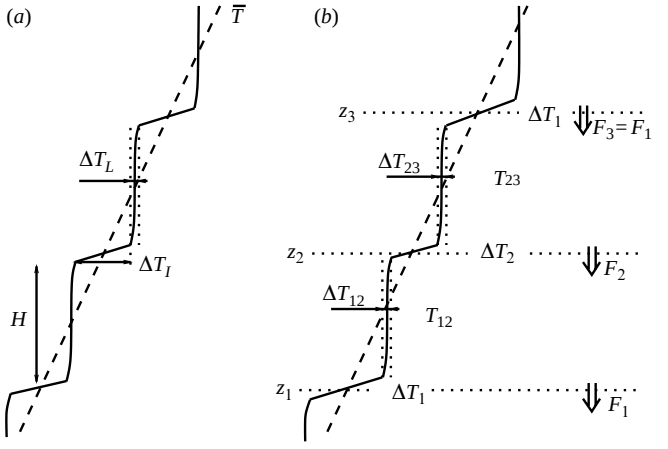

FIGURE 1. Schematic diagram illustrating the stability analysis for an infinite series of interfaces (modified from R03). (*a*) Basic state consisting of identical steps. (*b*) Perturbed state in which the T, S jumps at the even interfaces are slightly decreased, and the jumps at odd interfaces are increased.

2.1. *Flux laws*

To derive an analytical solution for the system in figure 1, the temperature and salinity fluxes have to be parameterized as a function of $(\Delta T, \Delta S)$ across the interfaces and convecting layers. The classical interfacial flux law (Turner 1967) is given by

$$\beta F_{S\,dim} = C_S(R)(\beta \Delta S_{dim})^b, \tag{1}$$

where $b = 4/3$, $F_{S\,dim}$ is the dimensional flux of salt, ΔS_{dim} is the dimensional salinity difference across the interface, and R is the density ratio. While the early laboratory experiments tended to support the 4/3 flux law (e.g. Schmitt 1979*a*) within the margins of the experimental and statistical error, questions have been raised with regard to its generality (Kelley *et al.* 2003). The laboratory values of C_S have been found to overestimate the oceanic fluxes by at least an order of magnitude, a discrepancy that may indicate that the effective exponent of the flux law realized in the oceanic conditions exceeds 4/3. Direct numerical simulations by Ozgokmen, Essenkov & Olson (1998) resulted in an approximate agreement with the 4/3 law over most of the explored parameter range, but with large deviations at high and low values of ΔS, whereas simulations in Paparella (2000) suggest that the exponent of the flux law consistently exceeds 4/3 and could be as high as $b = 2$. The reader is referred to Kunze (2003) for a discussion of these and other simple models of interfacial fluxes.

The situation with regard to the convective flux laws is somewhat similar. The early models – see the discussion in Emanuel (1994) – predicted that in turbulent Rayleigh–Bénard convection the Nusselt number Nu (defined as the ratio of the turbulent and molecular fluxes) is proportional to the Rayleigh number to the 1/3 power for stress-free boundaries (2/7 for no-slip). However, more recent studies raise doubts on the validity of the classical flux laws in the asymptotic limit of high Rayleigh number. A suite of laboratory and theoretical studies discussed and classified by Grossmann & Lohse (2000), demonstrates that, at least in the case of a single-component convection, the exponent of the convective flux law ($Nu \propto Ra^a$) is less than 1/3. Krishnamurti (1995), for example, reported the exponent $a = 0.2$ for an experiment in which the Rayleigh number was gradually increased from 10^6

and $a = 0.25$ when Ra was decreased. It is interesting to note that while the classical theories for the salt-finger interfaces are likely to underestimate the power of the flux law (1), the early predictions for thermal convection overestimate the corresponding exponent of the $Nu(Ra)$ relation.

The dynamics of the convection in thermohaline staircases is more complicated and much less studied than the Rayleigh–Bénard problem. An obvious difference between the two models results from the presence of two diffusing components. Convective overturning is driven by the density difference across the mixed layer, and therefore the dynamics of turbulent convection in this case is controlled by the density Rayleigh number

$$Ra_\rho = \frac{g}{k_T \nu} \frac{\Delta\rho}{\rho} H_{dim}^3, \tag{2}$$

rather than by the thermohaline Rayleigh number or Rayleigh numbers based on individual density components. Another complication is related to the connection conditions between layers and interfaces, which differ from the rigid boundaries in the Rayleigh–Bénard convection. Since our purpose is to illustrate the basic principle of staircase evolution rather than to make quantitative predictions, it is sensible to assume at the outset that the Rayleigh–Bénard dynamics has relevance to the convecting layers sandwiched between the salt-finger interfaces. Therefore, we use a flux law which is analogous to that in the simple one-component convection models:

$$Nu_L = \frac{F_{T\,dim} H_{dim}}{k_T \Delta T_{L\,dim}} = C_L Ra_\rho^a. \tag{3}$$

To be specific, we now consider an example with $a = 0.2$ in (3) and $b = 4/3$ in (1). Extension of the theory for generic power laws with arbitrary exponents a and b is presented in Appendix A.

2.2. *Basic state*

It is convenient to non-dimensionalize the governing equations using the salt-finger scales based on the overall temperature gradient $(\partial/\partial z)\bar{T}_{dim}$:

$$d = \left(\frac{k_T \nu}{g\alpha(\partial/\partial z)\bar{T}_{dim}} \right)^{1/4}$$

is the unit of length, d^2/k_T the time scale, and k_T/d the velocity scale. The expansion/contraction coefficients (α, β) are absorbed in (T, S), and $\alpha(\partial/\partial z)\bar{T}_{dim} d$ is used as the scale for both temperature and salinity. As a result, the interfacial flux law (1) reduces to

$$\left.\begin{aligned} F_T &= C(R_I)(\Delta T_I)^{4/3}, \\ F_S &= \frac{1}{\gamma(R_I)} F_T, \end{aligned}\right\} \tag{4}$$

where ΔT_I (ΔS_I) is the T (S) jump across the interface, $R_I = \Delta T_I / \Delta S_I$ the corresponding density ratio, and $\gamma(R_I)$ the flux ratio. The parameter $C(R_I)$ is related to the coefficient of the dimensional flux law (1) by $C = C_S \nu^{1/3} \gamma / (k_T^{2/3} g^{1/3} R_I^{4/3})$.

For the convecting layers, we use the flux law (3) with $a = 0.2$, which in our non-dimensional units reduces to

$$\left.\begin{aligned} F_T &= C_L \frac{\Delta T_L}{H} Ra_\rho^{0.2} = C_L (\Delta S_L - \Delta T_L)^{0.2} H^{-0.4} \Delta T_L, \\ F_S &= C_L (\Delta S_L - \Delta T_L)^{0.2} H^{-0.4} \Delta S_L = \frac{F_T}{R_L}, \end{aligned}\right\} \tag{5}$$

where ΔT_L, ΔS_L, and $R_L = \Delta T_L / \Delta S_L < 1$ pertain to the T, S variation across the

convecting layer. H is the height of the steps; the interfaces in our model are very thin, and therefore H is dominated by the contribution from the convecting layers. As is conventional for convectively generated turbulence, we assume that the eddy diffusivities of T and S in the mixed layers are equal.

Consider the system of identical layers and interfaces shown in figure 1(a). Existence of a steady state implies that the fluxes through the interfaces and layers are equal. Equating (4) and (5), we arrive at

$$\left.\begin{aligned} &C(R_I)(\Delta T_I)^{4/3} = C_L(\Delta S_L - \Delta T_L)^{0.2} H^{-0.4} \Delta T_L, \\ &\gamma(R_I) = R_L. \end{aligned}\right\} \tag{6}$$

The system (6) is closed by noting that

$$\left.\begin{aligned} &\Delta T_I + \Delta T_L = \bar{T}_z H = H, \\ &\Delta S_I + \Delta S_L = \bar{S}_z H = H/\bar{R}, \end{aligned}\right\} \tag{7}$$

which enables us to compute the temperature and salinity jumps across layers and interfaces as a function of the prescribed background T, S gradients and H. Of particular importance for the following theory is to establish a connection between the interfacial density ratio R_I and the background $\bar{R}$ that is based on the overall temperature and salinity gradients ($\bar{T}$, $\bar{S}$). While the general solution of (6) and (7) is deferred to § 3, it is useful at this point to consider briefly the asymptotic limit in which the (T, S) variation across the convecting layers is much less than the variation across the interfaces: $\Delta T_L \ll \Delta T_I$, $\Delta S_L \ll \Delta S_I$. After straightforward but lengthy algebra, we arrive at

$$\Delta R = R_I - \bar{R} = \bar{R}\left(\frac{\bar{R}}{\gamma} - 1\right)\left(\frac{C(\bar{R})}{C_L(\gamma^{-1} - 1)^{0.2}}\right)^{5/6} H^{4/9} + O\left(\frac{\Delta T_L^2}{\Delta T_I^2}\right), \tag{8}$$

which indicates that the inhomogeneity of the convective layers tends to increase the interfacial density ratio relative to its background value, and the difference between the two (ΔR) increases with H. The implications of this result for the stability properties of thermohaline staircases are profound; these are discussed in § 3.

2.3. *Linear stability analysis*

We now consider the perturbed staircase shown in figure 1(b). $T_{n\,n+1}$ denotes the temperature at the centre of a convecting layer bounded by the interfaces at $z = z_n$ and $z = z_{n+1}$, $\Delta T_{n\,n+1}$ is the temperature variation across this layer, and ΔT_n is the temperature jump across the nth interface (analogous notation is used for salinity). In time, temperature and salinity jumps across layers and interfaces may change, as may the distance between neighbouring interfaces. While both effects are realized in the oceanic and laboratory contexts, the vertical drift of the salt-finger interfaces is usually (e.g. McDougall 1991) related to the nonlinearity of the equation of state, which is beyond the scope of the present model. Thus, the distance between neighbouring interfaces is assumed constant.

Assuming that temperature and salinity profiles in the convecting layers are symmetric in z, as observed in laboratory and numerical experiments, the temperatures and salinities at their centres ($T_{n\,n+1}$, $S_{n\,n+1}$) also represent the layer-averaged values, and consequently

$$H(\partial/\partial t)T_{01} = F_{T1} - F_{T0}, \tag{9a}$$

$$H(\partial/\partial t)T_{12} = F_{T2} - F_{T1}, \tag{9b}$$

$$H(\partial/\partial t)T_{23} = F_{T3} - F_{T2}, \tag{9c}$$

where F_{Tn} is the downward heat flux across the interface at $z = z_n$. Next, we subtract (9a) from (9b), subtract (9b) from (9c), and simplify the results using the periodicity conditions $F_{T0} = F_{T2}$, $F_{T3} = F_{T1}$, $\Delta T_{01} = \Delta T_{23}$:

$$H(\partial/\partial t)[\Delta T_2 + 0.5(\Delta T_{12} + \Delta T_{23})] = 2(F_{T1} - F_{T2}), \tag{10a}$$

$$H(\partial/\partial t)[\Delta T_1 + 0.5(\Delta T_{12} + \Delta T_{23})] = -2(F_{T1} - F_{T2}). \tag{10b}$$

Subtracting (10b) from (10a), we arrive at

$$H\frac{\partial}{\partial t}(\Delta T_2 - \Delta T_1) = 4(F_{T1} - F_{T2}). \tag{11}$$

The flux law (4) reduces this expression to

$$H\frac{\partial}{\partial t}(\Delta T_2 - \Delta T_1) = 4\left(C(R_1)\Delta T_1^{4/3} - C(R_2)\Delta T_2^{4/3}\right), \tag{12}$$

where $R_n = \Delta T_n/\Delta S_n$, and the corresponding salinity equation is

$$H\frac{\partial}{\partial t}(\Delta S_2 - \Delta S_1) = 4\left(\frac{C(R_1)}{\gamma(R_1)}\Delta T_1^{4/3} - \frac{C(R_2)}{\gamma(R_2)}\Delta T_2^{4/3}\right). \tag{13}$$

Note that the temperature and salinity jumps across the mixed layers do not appear explicitly in relations (12) and (13). Thus, the interfacial dynamics described by this system is decoupled from convection in the mixed layers, which is rather remarkable since here (ΔT_{nn+1}, ΔS_{nn+1}) are not necessarily small.

We now simplify our key relations (12) and (13) by introducing the following variables:

$$A = \frac{\Delta T_2 - \Delta T_1}{\Delta T_I}, \qquad B = \frac{\Delta S_2 - \Delta S_1}{\Delta S_I},$$

which represent the relative amplitude of the 'merging' perturbation in figure 1(b). In order to perform a linear stability analysis of the steady state in figure 1(a), we consider $A, B \ll 1$ and linearize (12) and (13) retaining only the order-(A, B) terms. The resulting linear system for A and B is

$$H\Delta T_I\frac{\partial}{\partial t}A = -4\left(\left.\frac{\partial C}{\partial R}\right|_{R=R_I} R_I(A-B) + \frac{4}{3}C(R_I)A\right)\Delta T_I^{4/3},$$

$$H\Delta S_I\frac{\partial}{\partial t}B = -4\left(\frac{1}{\gamma(R_I)}\left.\frac{\partial C}{\partial R}\right|_{R=R_I} R_I(A-B) + \frac{4}{3}\frac{C(R_I)}{\gamma(R_I)}A + C(R_I)\left.\frac{\partial(1/\gamma)}{\partial R}\right|_{R=R_I} R_I(A-B)\right)\Delta T_I^{4/3},$$

and substitution of the normal modes $(A, B) = (A_0, B_0)\exp(\lambda t)$ yields the eigenvalue equation for growth rates:

$$\lambda^2 + \frac{4\Delta T_I^{1/3}}{H}\left[\frac{4}{3}C(R_I) + D_2 - \frac{R_I D_2}{\gamma(R_I)} - D_1 C(R_I)R_I\right]\lambda - \frac{64\Delta T_I^{2/3}}{3H^2}C^2(R_I)D_1 R_I = 0, \tag{14}$$

where

$$D_1 = \left.\frac{\partial(1/\gamma)}{\partial R}\right|_{R=R_I} R_I, \qquad D_2 = \left.\frac{\partial C}{\partial R}\right|_{R=R_I} R_I.$$

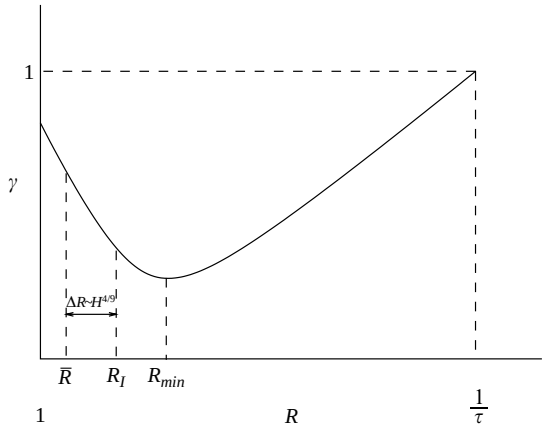

FIGURE 2. Dependence of the flux ratio on the interfacial density ratio R_I. Thickening of layers tends to increase R_I and decrease γ (see the text).

The eigenvalue equation (14) suggests the following simple condition for instability. If $\gamma(R)$ is a decreasing function of R in the vicinity of $R = R_I$, then $D_1 > 0$. Hence, the free coefficient of the quadratic eigenvalue equation is negative, and therefore (14) has two real roots of opposite sign. Existence of a positive eigenvalue implies the instability of the basic field and suggests that 'strong' interfaces, characterized by larger $(\Delta T, \Delta S)$, grow further at the expense of weaker interfaces. The weaker interfaces gradually erode and, we argue, eventually disappear, which increases the average vertical scale of layers. On the other hand, if $D_1 < 0$, both roots of the eigenvalue equation (14) are negative, provided that the heat flux decreases with the density ratio ($D_2 < 0$), and the basic state in figure 1(*a*) is stable.

Before we discuss in the next section the consequences of this instability, it should be emphasized that our key instability condition

$$\left.\frac{\partial \gamma}{\partial R}\right|_{R=R_I} < 0 \tag{15}$$

does not depend on the specific interfacial flux law, and different formulations (see Appendix A) would yield the same result as long as F_T increases with ΔT.

3. The equilibrium height of layers

The eigenvalue equation (14) indicates that the stability of the thermohaline staircase is controlled by the patterns of the flux law coefficient $C(R)$ and the flux ratio $\gamma(R)$. Their qualitative behaviour is known from numerous laboratory experiments (e.g. Griffiths & Ruddick 1980), numerical simulations (Stern, Radko & Simeonov 2001), oceanic measurements (St. Laurent & Schmitt 1999), and theoretical models (Schmitt 1979*b*; Radko & Stern 2000). $C(R)$ is a decreasing function of R, which reflects the tendency of double-diffusion to intensify on moving away from the marginal instability point $R = 1/\tau$ (where $\tau = k_S/k_T$ is the Lewis number). Detailed discussion of the dependence of the flux ratio γ on R, based on the theoretical reasoning and observational evidence, is given in Appendix B. Here we emphasize that the flux ratio is non-monotonic; its variation as a function of R is shown schematically in figure 2. As R is decreased from $1/\tau$, γ first decreases, reaching its minimum value

at a point (R_{min}) in the interior of the salt-finger interval $1 < R_{min} < 1/\tau$, and then increases – a pattern that can be rationalized by considering fluxes in the linearly fastest growing fingers (Schmitt 1979*b*). Schmitt's model suggests that the flux ratio rapidly decreases with R in the range $1 < R < 2$, remains nearly constant for $2 < R < 8$, where $\gamma \approx \gamma_{min} \approx 0.6$, and then gently increases to reach unity at $R = 1/\tau \approx 100$. In our theory we concentrate on the sufficiently low values of density ratio $R < 2$ that favour spontaneous layer formation (R03), and approximate the $\gamma(R)$ relation there by the following simple analytical function:

$$\gamma(R) = 0.6 + \frac{(R - R_{min})^2}{2.5}, \qquad R_{min} = 2. \tag{16}$$

In the scenario of layering advocated by R03, transition from a smooth gradient to the equilibrated staircase begins with the formation of very thin layers, only a few salt fingers in height. This is a consequence of the ultraviolet catastrophe in the instability of the flux gradient laws – the linear growth rate of the unstable mode increases with wavenumber. The layers then undergo a series of merging events, which increase the average height of layers. The instability condition (15) suggests that the merger of layers persists for as long as $R_I < R_{min}$. According to (8), thickening of layers, in turn, increases the interfacial density ratio R_I. Thus, eventually R_I reaches R_{min}, at which point the system of layers becomes stable, and the coarsening stops (see the schematic in figure 2). The critical condition

$$R_I(H_0) = R_{min}, \tag{17}$$

implicitly determines H_0. Combining (6) and (7) with the condition that $\Delta T_I / \Delta S_I = R_I = R_{min}$ for $H = H_0$ results in a system of five equations with five unknowns (T_I, T_L, S_I, S_L, H_0), which is readily solved for $H_0(\bar{R})$:

$$H_0 = \left(\frac{C_L}{C(R_{min})}\right)^{15/8} \frac{(R_{min}/\bar{R} - 1)^{9/4} (R_{min}/\gamma_{min} - 1)^{1/4}}{(R_{min}/\gamma_{min} - R_{min}/\bar{R})^{5/2}} \left(\frac{1}{\gamma_{min}} - 1\right)^{3/8}, \tag{18}$$

which is the expression sought for the thickness of layers in a fully equilibrated staircase.†

It is important now to determine whether our theory (18) is capable of predicting the correct order of magnitude for the step heights (H_0) in the ocean. For that, we have to specify the coefficients of the interfacial and convective flux laws [$C(R_{min})$ and C_L]. The most recent and reliable estimate of fluxes in the tropical North Atlantic (C-SALT staircase) came as a result of the Salt Finger Tracer Release Experiment (Schmitt *et al.* 2004). The observed overall salt eddy diffusivity of $K_S = 0.9\,\mathrm{cm^2\,s^{-1}}$ corresponds to $\beta F_{S\,dim} = (K_S \beta \bar{S}_z)_{dim} \approx 3 \times 10^{-10}\,\mathrm{m\,s^{-1}}$ and $\alpha F_{T\,dim} = \gamma \beta F_{S\,dim} \approx 2 \times 10^{-10}\,\mathrm{m\,s^{-1}}$. Using the representative $\Delta S_{I\,dim} = 0.07$ p.p.t. in (1) we arrive at $C_S \sim 1.5 \times 10^{-4}\,\mathrm{m\,s^{-1}}$, which translates to non-dimensional $C(R_{min}) = 0.01$. (Note that this number is less, by an order of magnitude, than the values realized in the laboratory experiments, as discussed in § 2.1.)

The convective flux law for oceanic staircases is more difficult to calibrate, since temperature and salinity differences across the mixed layers are small and unsteady. Furthermore, most of the z-variation in T and S occurs in the thin sublayers that connect convecting regions with interfaces; the interior of layers is almost

† One can readily recognize that (18) is directly related to the interfacial density ratio equation (8). While (8) was derived (§ 2) by expanding the governing equations in $\Delta T_L / \Delta T_I$, it can be recovered from (18) by substituting R_I for R_{min} and using $R_I \approx \bar{R}$.

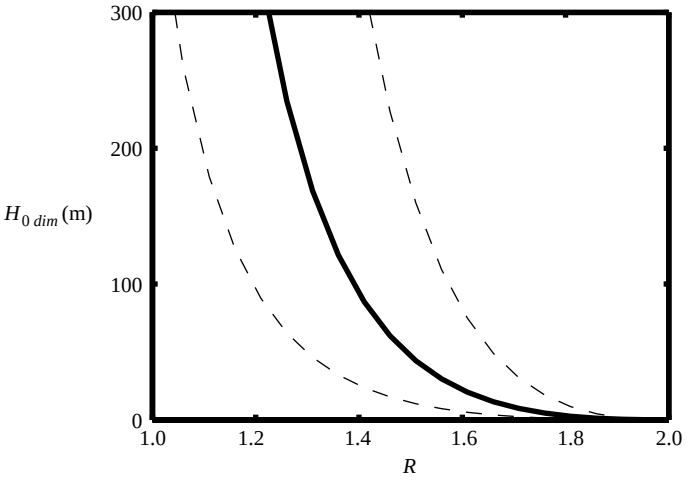

FIGURE 3. The dimensional equilibrium layer thickness as a function of the background density ratio $\bar{R}$ for a fixed background temperature gradient of $(\partial/\partial z)\bar{T}_{dim} = 0.03^{\circ}\,\mathrm{m}^{-1}$. Solid curve corresponds to $C_L/C = 10^3$, whereas the lower (upper) dashed curve is for $C_L/C = 500$ ($C_L/C = 2 \times 10^3$).

homogeneous. However, William Merryfield (private communication) pointed out that the scale of ΔT_L can be estimated from the temperature inhomogeneities in the convective plumes measured by Marmorino, Brown & Morris (1987). Their figure 4 shows a relatively thin C-SALT layer ($H_{dim} \approx 8$ m) with alternating plumes of cold light water rising from the lower interface and warm dense plumes descending from above. A temperature trace through the middle of this layer reveals temperature variations of $\sim 0.01\,^{\circ}$C, but much larger contrasts are observed in the thermal boundary sublayers; visual inspection of figure 4 in Marmorino *et al.* (1987) suggests $\Delta T_L \sim 0.03\,^{\circ}$C. Using the second equation in (6), we estimate $\Delta\rho_L/\rho = (1/\gamma - 1)\alpha\Delta T_L \approx 4 \times 10^{-6}$, which results in

$$Ra_\rho = \frac{g}{k_T \nu}\frac{\Delta\rho_L}{\rho}H_{dim}^3 \approx 1.5 \times 10^{11}, \quad Nu_L = \frac{\alpha F_{T\,dim} H_{dim}}{k_T \alpha \Delta T_{L\,dim}} \approx 2 \times 10^3,$$

and therefore the coefficient of the convective flux law (3) is $C_L \sim 10$.

To compare the prediction (18) with oceanographic observations, we now revert to the dimensional thickness

$$H_{0\,dim} = H_0\left(\frac{\nu k_T}{g\alpha(\partial/\partial z)\bar{T}_{dim}}\right)^{1/4},$$

which is plotted (heavy solid line) in figure 3 as a function of the background density ratio for fixed $(\partial/\partial z)\bar{T}_{dim} = 0.03^{\circ}\,\mathrm{m}^{-1}$ and $C_L/C = 10/0.01 = 10^3$. The range of layer heights in figure 3 (0–300 m) is generally consistent with observations, and so is the tendency for layers to thicken at low $\bar{R}$. For $\bar{R} = 1.6$, for example, our model predicts the scale of 20 m, which is close to the thickness of layers observed in the tropical North Atlantic, whereas very thick layers with $H_{0\,dim} \sim 300$ m and more are often observed in the Tyrrhenian Sea (see Zodiatis & Gasparini 1996) where the density ratio is anomalously low ($\bar{R} \approx 1.2$). It should be noted, however, that (18) strongly depends on the ratio C_L/C, whose value is poorly constrained by oceanographic measurements, and therefore in figure 3 we also show the $H_{0\,dim}(\bar{R})$ relations (dashed curves) for $C_L/C = 500$ and $C_L/C = 2 \times 10^3$.

4. Numerical simulations

In order to determine the extent to which the merging conditions suggested by the foregoing linear analysis are applicable to a system of layers that are not necessarily close in size and strength, we now turn to a fully nonlinear numerical model. The following calculation describes the evolution of the temperature and salinity fields averaged over spatial/time scales that greatly exceed those for individual salt fingers.

4.1. *Parameterized gradient flux laws*

The continuous one-dimensional large-scale T, S equations in flux form are

$$\frac{\partial T}{\partial t} = \frac{\partial}{\partial z} F_T, \quad \frac{\partial S}{\partial t} = \frac{\partial}{\partial z} F_S, \tag{19}$$

where (F_T, F_S) are the downward (i.e. positive) temperature and salinity fluxes, and (T, S) represent the local modification of the uniform background gradients. The total large-scale temperature and salinity fields are therefore given by $T_{total} = z + T$, $S_{total} = z/\bar{R} + S$.

For the salt-finger regions, where density increases with depth, we assume, following R03, that fluxes depend only on local large-scale gradients:

$$\left.\begin{aligned} F_T &= Nu(R)\frac{\partial T_{total}}{\partial z} \\ F_S &= \frac{1}{\gamma(R)} F_T \end{aligned}\right\} \quad \text{for } \frac{\partial \rho_{total}}{\partial z} < 0 \tag{20}$$

where the non-dimensional parameters γ and $Nu > 0$ are the flux ratio and the Nusselt number respectively; these are determined by the local density ratio (see the discussion in R03)

$$R = \frac{(\partial/\partial z)T_{total}}{(\partial/\partial z)S_{total}} = \frac{1 + (\partial/\partial z)T}{1/\bar{R} + (\partial/\partial z)S}.$$

A simple analytical function, consistent with the direct numerical simulations in Stern *et al.* (2001), is used for the Nusselt number:

$$Nu(R) = \frac{50}{R - 1}, \tag{21}$$

and the $\gamma(R)$ relation is given in (16). In what follows the gradient flux formulation (20) will be applied locally to the interfaces in a staircase and related to the interfacial flux laws used in our analytical theory.

Different physics, however, applies to the convective regions, where the averaged density decreases with depth. As assumed in (3), the magnitude of fluxes there is determined by the density Rayleigh number (2) based on the height of a density inversion, which is reflected in the following closure:

$$\left.\begin{aligned} F_T &= Nu_L \frac{\partial T_{total}}{\partial z} = C_L Ra_\rho^{0.2} \frac{\partial T_{total}}{\partial z} \\ F_S &= C_L Ra_\rho^{0.2} \frac{\partial S_{total}}{\partial z} \end{aligned}\right\} \quad \text{for } \frac{\partial \rho_{total}}{\partial z} > 0. \tag{22}$$

The parameterization in (22) clearly oversimplifies the dynamics of convection. Since the eddy diffusivity in the model ($K = C_L Ra_\rho^{0.2}$) is spatially uniform within the layers, the resulting temperature and salinity profiles are linear. Thus, our solutions cannot describe certain distinctive features of turbulent convection, such as the presence of thin stratified sublayers at the edges of the convecting zones or a relatively

homogeneous interior. However, this model correctly represents the integral properties of convection, particularly the dependence of fluxes on layer height and density variation. These are the characteristics that actually control the evolution of the thermohaline staircase in time, which justifies use of the parameterization in (22) as a zero-order description of the physics and dynamics at play.

4.2. *Model solutions*

A major difficulty in treating the parameterized salt-finger equations (19) and (20) is related to the properties of the layer-forming instability of smooth temperature and salinity gradients (γ-instability in R03). As shown in R03, this instability is characterized by the increase and divergence of the growth rate as the wavenumber of disturbances increases, implying that the problem is mathematically ill-posed. However, this ultraviolet catastrophe in the model may be unphysical, since the stability analysis itself is valid only for scales that exceed the characteristic salt-finger width. Direct numerical simulations in R03 show that the layers formed first on the uniform basic gradient are a few ($\sim$10) salt fingers in height, which suggests that higher harmonics are damped by the processes that are beyond the scope of our theory. In order to surmount the problem of ill-posedness, the governing equations (19) are modified by adding the hyperdiffusion terms as follows:

$$\frac{\partial T}{\partial t} = \frac{\partial}{\partial z} F_T - \mu \frac{\partial^4}{\partial z^4} T, \quad \frac{\partial S}{\partial t} = \frac{\partial}{\partial z} F_S - \mu \frac{\partial^4}{\partial z^4} S, \tag{23}$$

which suppresses the growth of small-scale modes in the numerical model, but has little effect on scales that significantly exceed the characteristic salt-finger width. For simplicity, we use a spatially uniform hyperdiffusivity μ.

We impose the periodic boundary conditions for (T, S) at the ends of the computational interval ($z = 0, L_z$), and the system of equations (20), (22) and (23) is solved numerically using a pseudospectral method analogous to that employed in Radko & Stern (2000). In the following calculation $\bar{R} = 1.6$, and the height of the computational domain is $L_z = 14\,800$, which corresponds to the dimensional height of approximately 100 m, resolved by $N_z = 1024$ elements. As previously, $C_L = 10$. The model is initiated by uniform temperature and salinity gradients slightly perturbed by the linearly fastest-growing unstable mode of equations (20) and (23). The dissipation parameter $\mu = 5 \times 10^4$ is chosen such that the wavelength of this mode exceeds the width of the fastest-growing individual fingers by an order of magnitude, as suggested by the direct numerical simulations in R03.

Figure 4 presents the evolution in time of the temperature profile $T_{total}(z)$. The first stage is characterized by the monotonic growth of the unstable normal mode. Modification of the initial temperature distribution by the γ-instability at $t = 80$ is shown in figure 4(*a*). By $t = 400$ (figure 4*b*), the amplitude of the perturbation becomes sufficient to create numerous density inversions, where the fluxes are controlled by the convective closure (22). Figure 4(*c–e*) illustrates the change in the evolutionary pattern associated with the formation of a well-defined staircase: the steps start to merge continuously. Merging occurs when sufficiently strong interfaces, characterized by large temperature and salinity jumps, grow further, while weaker interfaces decay and eventually disappear, in accord with predictions of the linear theory in §§2,3. The number of layers decreases and their characteristic vertical scale increases correspondingly. As expected, the interfaces do not drift vertically. However, as time progresses, the coarsening of layers becomes less rapid and eventually stops completely. No visible changes in the temperature field occur between $t = 2.5 \times 10^5$

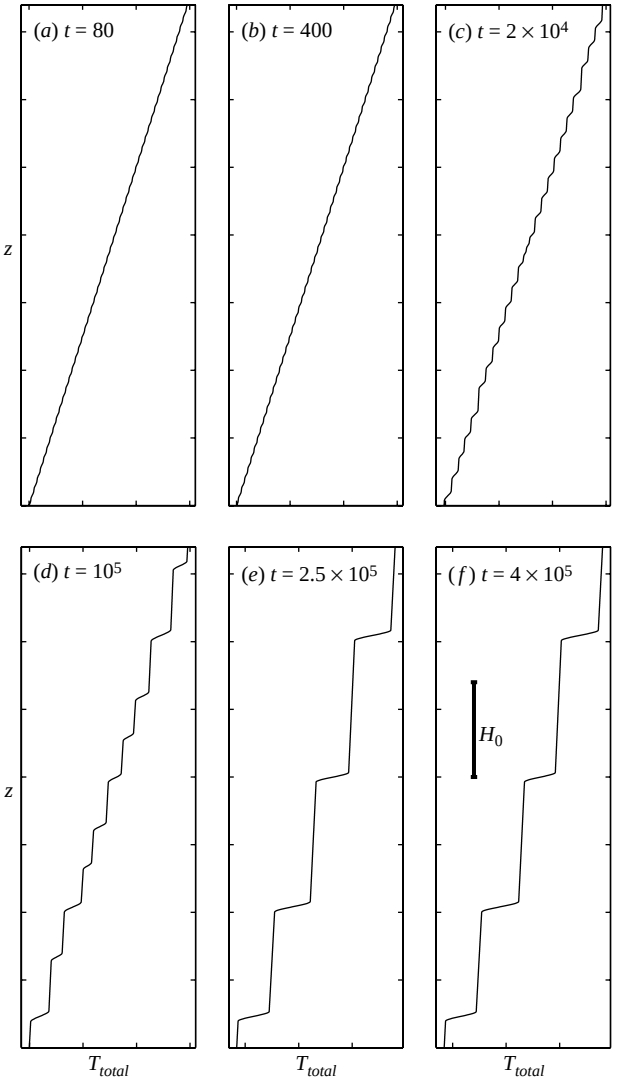

FIGURE 4. Formation and evolution of layers in the numerical experiment. The total temperature profiles are shown at $(a–f)$ $t = 80$, 400, 2×10^4, 1×10^5, 2.5×10^5, 4×10^5. Note the appearance of the convecting layers separated by thin stratified interfaces at $t = 400$, followed by a series of merging events, and their eventual equilibration.

in figure 4(e) and $t = 4 \times 10^5$ in figure 4(f), suggesting that the staircase reaches a stable steady state. Note that the period of equilibration in figure 4 is remarkably long (relative to the finger time scale),

$$t_{dim} \sim 2.5 \times 10^5 \left(\frac{\nu}{g k_T \alpha (\partial/\partial z) \bar{T}_{dim}} \right)^{1/2} \approx 2.5 \text{ years}.$$

Such a slow predicted evolution of thermohaline staircases by merger is supported by some of the oceanographic observations – see, for example, figure 11(a, b) in Zodiatis & Gasparini (1996) for the Tyrrhenian staircase.

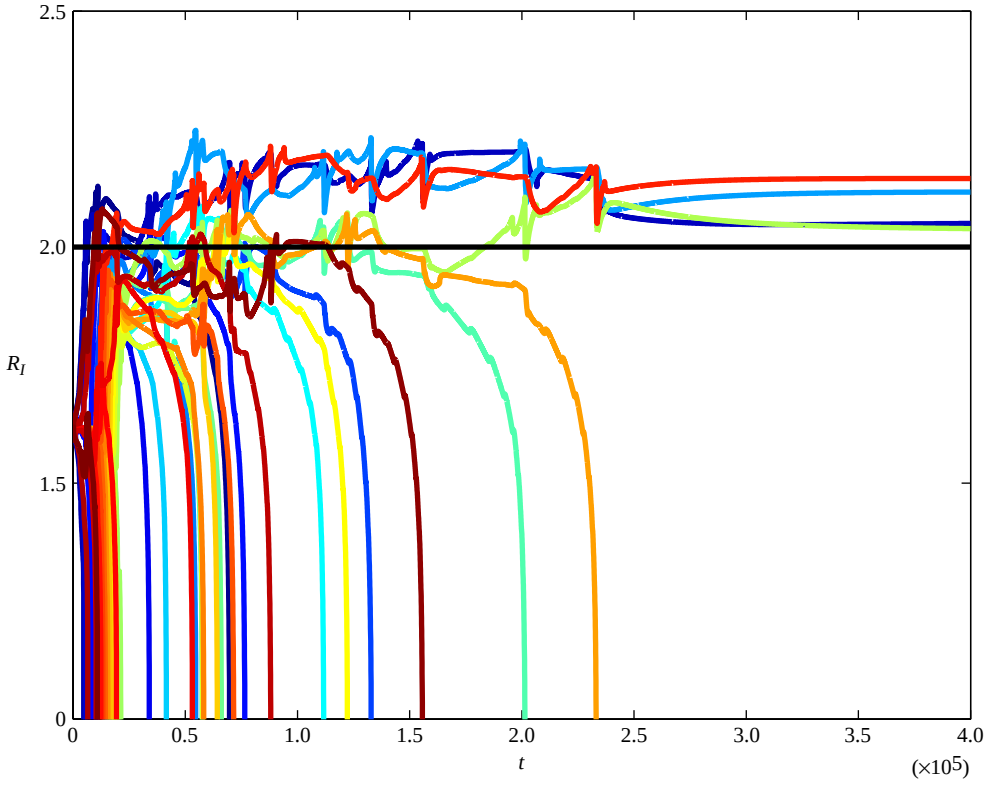

FIGURE 5. Evolution of the interfacial density ratios (R_I) in time. Note the drift towards higher values of R_I, which stabilizes the staircase; the boundary of the stable zone $R_I > R_{min} = 2$ is indicated by the straight horizontal line.

The equilibration of a staircase in the analytical theory (§§2,3) was attributed to the fact that interfacial density ratios approach a critical value R_{min}, where $\partial\gamma/\partial R$ changes sign. To confirm that this effect is responsible for arresting the coarsening of layers in the foregoing numerical simulation, we plot in figure 5 the interfacial density ratios at various times. These are computed numerically from variations in T and S across regions with negative density gradient. As layers merge, the interfacial density ratios drift towards higher values, which tends to suppress the merging instability. Finally, at $t = 2.5 \times 10^5$, all interfacial density ratios enter the stable zone $R_I \gtrsim R_{min} = 2$, and the merging stops.†

Diagnostics in figure 5 indicate that our numerical simulation does reproduce the mechanism of equilibration predicted by the linear model in §§2,3. It remains to be shown that the equilibrium height realized in the numerical model is also consistent with the theoretical prediction; to do that, we first derive the interfacial flux law realized in the numerical model. Scaling analysis of the salt-finger equations (23) indicates that the characteristic thickness of the interfaces h in the model is controlled by the dissipation parameter μ, and therefore $h = h(R_I, \mu)$, independent of the jumps in the individual density components across the interface. According to (20) and (21),

† Note that because of the nonlinearity of the governing equations, the interfacial $\gamma_I(R_I)$ relation is slightly different from the local $\gamma(R)$ relation (16) assumed for the interior of the interfaces. The stability of a staircase is of course controlled by the pattern of the interfacial flux ratio $\gamma_I(R_I)$.

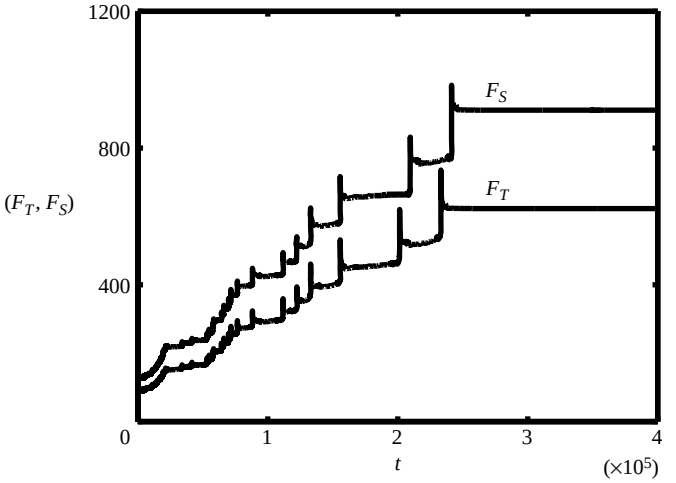

FIGURE 6. The non-dimensional downward fluxes of heat and salt as a function of time for the calculation in figure 4. Formation and merger of layers is accompanied by a significant increase in fluxes.

the temperature flux is

$$F_T \propto \frac{\Delta T_I}{h} Nu(R_I) = C(R)\Delta T_I. \tag{24}$$

Thus, our numerical simulation corresponds to the case in which the exponents (a, b) of the power laws (A 1) for convection and salt fingering, discussed in Appendix A, are

$$a = 0.2, \qquad b = 1, \tag{25}$$

that is, slightly different from our central example in §§ 2,3 with $(a, b) = (0.2, 4/3)$. This form of the interfacial flux law (24) is a consequence of the assumed parameterization (23) in which the dissipation parameter μ is constant; the conventional 4/3 flux law can be recovered by introducing a more complicated model (not shown) with spatially varying μ which is set by the local, rather than overall, temperature/salinity gradients.

The coefficient of the flux law (24) is calibrated from the numerical simulation in figure 4. For R_I approaching R_{min}, its value is $C = 0.18$, and the expression for equilibrium thickness derived in Appendix A (A 4) yields

$$H_0 = 2.8 \times 10^3. \tag{26}$$

This value is close to the thickness realized in the numerical model – the theoretical scale is indicated in figure 4(f) by a heavy vertical line. In dimensional units, (26) corresponds to $H_{0\,dim} \sim 20$ m, which is consistent with the observed thickness of oceanic layers for $\bar{R} = 1.6$ (Schmitt 1981).

It is also interesting to examine how the staircase formation and evolution affects temperature and salinity fluxes. Figure 6 gives the time record of the z-averaged fluxes for the experiment in figure 4, which indicates that the merger events are accompanied by significant increase in fluxes. Overall, formation and equilibration of the staircase changes the fluxes by almost an order of magnitude relative to that on a uniform gradient. Corresponding dimensional eddy diffusivities increase from $K_T = 0.12\,\mathrm{cm^2\,s^{-1}}$ to $K_T = 0.9\,\mathrm{cm^2\,s^{-1}}$ for heat, and from $K_S = 0.25\,\mathrm{cm^2\,s^{-1}}$ to $K_S = 2\,\mathrm{cm^2\,s^{-1}}$ for salt. These diffusivities are comparable (within a factor of two) to

the values suggested by oceanographic microstructure and tracer release measurements in a smooth T, S gradient (Ledwell, Watson & Law 1993) and in a thermohaline staircase (Schmitt *et al.* 2004).

Finally, to test the sensitivity of our results to the assumed value of the dissipation parameter μ, we have also performed an experiment in which μ was reduced by a factor of two (to $\mu = 2.5 \times 10^4$). The average step height in the equilibrated staircase decreased to $H_{0\,dim} = 15$ m, the equilibration period reduced to one year, and the final eddy diffusivities became $K_T = 0.6\,\mathrm{cm^2\,s^{-1}}$, $K_S = 1.4\,\mathrm{cm^2\,s^{-1}}$.

5. Discussion

In this paper we have studied the dynamics of layers and interfaces in a double-diffusive fluid using a theoretical model and numerical simulations. The evolution of the initially uniform temperature and salinity gradients into an equilibrated staircase can be divided into three distinct stages. The first features to emerge are related to the instability of the salt-finger gradient flux laws. Unstable perturbations grow monotonically and eventually transform the basic gradient into a stepped structure consisting of salt-finger interfaces sandwiched between convecting layers. Layers that form first are thin and unsteady. The next evolutionary stage consists of a series of merging events, in which strong interfaces, characterized by large temperature and salinity jumps, grow further at the expense of weaker interfaces that gradually erode and eventually disappear. The characteristic size of steps correspondingly increases in time.

The final stage involves the equilibration of a staircase when layers become sufficiently thick. This is explained by the linear stability analysis for a series of identical interfaces, which reveals a tendency for layers to merge if their height (H) is less than the critical value (H_0) and to remain steady if H exceeds H_0. The existence of a long-wave cut-off scale for the merging instability is related to the slight inhomogeneity of the convecting layers, which has a stabilizing effect on the thermohaline staircase. The predicted equilibrium scale of steps ($\sim$20 m for the density ratio of $\bar{R} = 1.6$) is consistent with oceanographic observations, and inferences from the linear instability theory are supported by fully nonlinear numerical simulations in § 4.

Although our specific solutions depend on the interfacial and convective flux laws, which are not well-known in the oceanographic context, some features are robust and not model dependent. In particular, there are a number of theoretical predictions for equilibrated staircases that are testable against the observations and laboratory experiments. These include the following:

1. The local density ratio in the salt-finger interfaces significantly exceeds the background density ratio.

2. The flux ratio in staircases is spatially uniform and equals the minimum value $\gamma_I = \min_R[\gamma(R)]$.

3. The height of steps sharply decreases with the density ratio but only weakly depends on the background temperature gradient.

Some existing observational evidence already tends to support these aspects of our theory. The anticorrelation of the step heights with $\bar{R}$ is particularly conspicuous for layers within the same staircase (see, for example, table 1 in Zodiatis & Gasparini 1996) but can also be noticed by comparing the different staircases (Schmitt 1981). The strikingly uniform apparent flux convergence ratio noted by Schmitt *et al.* (1987) may also be directly related to the predicted uniformity of γ in the fully equilibrated

staircases. However, more measurements and data analysis focusing on equilibrium balances would be needed to prove unequivocally that the predicted dynamics is realized in oceanic conditions.

It is also important to note that many features of double-diffusive layering are very similar to those for turbulent one-component fluids (e.g. Balmforth, Llewellyn Smith & Young 1998). These include the formation of thin layers as a result of flux-law instabilities and their subsequent coarsening. However, the layer merger events in Balmforth *et al.*'s theory continue indefinitely, which indicates that the one-component model does not include the dynamics required to explain the finite vertical scale of the oceanic steps. Thus, the key strength of our model is related to its ability to describe the processes that arrest the coarsening of layers and thereby determine their equilibrium thickness.

Support of the National Science Foundation is gratefully acknowledged. The author thanks Jim Ledwell, William Merryfield, Ray Schmitt, Melvin Stern and George Veronis for helpful comments.

Appendix A. Generalization of the analytical theory

While the stability analysis in §§2,3 was based on the specific parameterizations of the convection and salt fingering in (4) and (5), it is straightforward to extend our theory to the more general flux laws given by

$$\left.\begin{aligned} F_T &= C_L \frac{\Delta T_L}{H} Ra_\rho^a, \qquad \text{for layers,} \\ F_T &= C(R_I)(\Delta T_I)^b, \qquad \text{for interfaces,} \end{aligned}\right\} \tag{A 1}$$

where a and b are the arbitrary positive numbers. Generalization of the asymptotic expression (8) yields

$$\Delta R = R_I - \bar{R} = \bar{R}\left(\frac{\bar{R}}{\gamma} - 1\right)\left[\frac{C(\bar{R})}{C_L(\gamma^{-1}-1)^a}\right]^{\frac{1}{1+a}} H^{\frac{b-4a}{a+1}} + O\left(\frac{\Delta T_L^2}{\Delta T_I^2}\right),$$

which implies that the coarsening of layers is accompanied by an increase of the interfacial density ratio, provided that

$$b > 4a. \tag{A 2}$$

The existing evidence (see the discussion in §2.1) indicates that the flux laws realized in the thermohaline staircases do satisfy the consistency condition in (A 2).

Reproducing the linear stability analysis in §2.3 for the interfacial flux law in (A 1) yields the following equation for growth rates:

$$\lambda^2 + \frac{4\Delta T_I^{b-1}}{H}\left[bC(R_I) + D_2 - \frac{R_I D_2}{\gamma(R_I)} - D_1 C(R_I) R_I\right]\lambda - \frac{16b\Delta T_I^{2b-2}}{H^2} C^2(R_I) D_1 R_I = 0. \tag{A 3}$$

Clearly, the previously used eigenvalue equation (14) is a particular case of (A 3) for $b = 4/3$, and, as long as $b > 0$, the instability condition (15) in §2 is valid in the general case as well. If $R < R_{min}$, then

$$D_1 = \left.\frac{\partial(1/\gamma)}{\partial R}\right|_{R=R_I} R_I > 0,$$

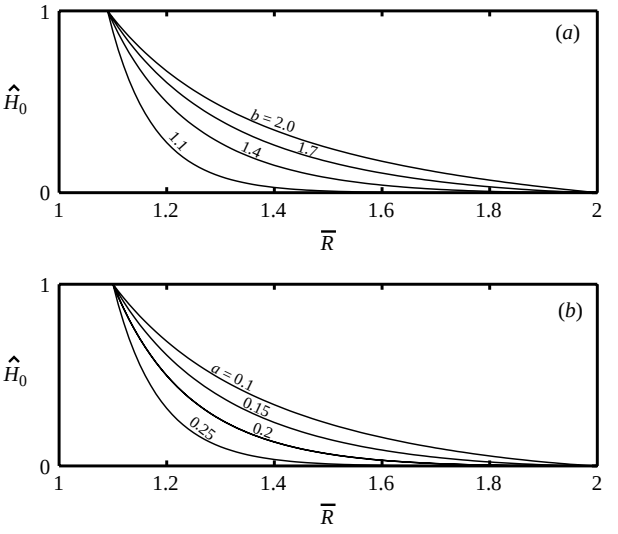

FIGURE 7. Dependence of the layer thickness (normalized by its value at $\bar{R}=1.1$) on the background density ratio ($\bar{R}$). (*a*) The patterns of $\hat{H}_0(\bar{R})$ for a fixed exponent of the convective flux law $a=0.2$ and various exponents of the interfacial flux law b; in (*b*) we use a fixed $b=4/3$ and different values of a.

and (A 3) has two real roots of opposite sign. Existence of a positive eigenvalue implies the instability of a basic state, which manifests itself in a spontaneous merger of sufficiently thin layers.

Finally, the counterpart of (18) for the equilibrium thickness of layers is now

$$H_0 = \left(\frac{C_L}{C(R_{min})}\right)^{\frac{1}{b-4a}} \frac{\left(R_{min}/\bar{R}-1\right)^{\frac{a+1}{b-4a}} \left(R_{min}/\gamma_{min}-1\right)^{\frac{b-a-1}{b-4a}}}{\left(R_{min}/\gamma_{min}-R_{min}/\bar{R}\right)^{\frac{b}{b-4a}}} \left(\frac{1}{\gamma_{min}}-1\right)^{\frac{a}{b-4a}}. \qquad \text{(A 4)}$$

The interpretation of (A 4) is greatly complicated by the uncertainty in the specific values of the prefactors C and C_L which control the amplitude of H_0. To examine the general character of the dependence of layer thickness on the density ratio for various a and b, we normalize $H_0(\bar{R})$ in (A 4) by its value at $\bar{R}=1.1$ and plot $\hat{H}_0 = H_0(\bar{R})/H_0(1.1)$ as a function of $\bar{R}$ in figure 7. All resulting $\hat{H}_0(\bar{R})$ curves are qualitatively similar and characterized by a sharp decrease of layer thickness with $\bar{R}$.

Appendix B. Dependence of the flux ratio (γ) on the density ratio (R)

Because of its critical role in the theory of layer formation (§ 3), we now review some known (e.g. Kunze 2003) properties of the $\gamma(R)$ relation in the salt-finger parameter range $1<R<1/\tau$.

The heat/salt buoyancy flux ratio $\gamma=\alpha F_{T\,dim}/\beta F_{S\,dim}$ is one of the most stable characteristics of active double diffusion whose value is strongly constrained by the energy requirements. Consider first the situation in which the vertical mixing is driven entirely by the salt fingers, as occurs in most laboratory and numerical experiments. The flux ratio in this case has to be less than unity to satisfy the energy balance. That is, the density flux of heat cannot exceed the oppositely signed density flux of salt;

	$R_{min}=1.7$	$R_{min}=2$	$R_{min}=2.5$
$\bar{R}=1.2$	172	350	640
$\bar{R}=1.4$	28	93	224
$\bar{R}=1.6$	1.4	22	84

TABLE 1. Theoretical prediction of the equilibrium layer thickness $H_{0\,dim}$ in m for various $\bar{R}$ and R_{min}; other parameters are the same as in figure 3.

it is the difference between the potential energy lost by the salt component and the energy gained by the thermal stratification that drives the fingering flow, eventually dissipating as kinetic energy.

However, as the marginal stability point is approached ($R \to 1/\tau$), heat flux becomes close to the flux of salt, fingering weakens and stops completely at $R = 1/\tau$. The corresponding increase of the flux ratio towards unity has been observed in the direct numerical simulations (Stern & Radko 1998; Radko & Stern 1999) and can be rationalized by linear (Schmitt 1979*b*) and weakly nonlinear analysis (Radko & Stern 1999, 2000). It is also sensible to assume that the flux ratio reaches unity at the opposite end of the salt-finger interval ($R = 1$). For $R < 1$, the system becomes top-heavy and therefore convectively unstable. The fully developed convection is characterized by nearly equal diffusivities of the density components and passive tracers. Hence, $\gamma = R$ for $R < 1$ and, unless $\gamma(R)$ is discontinuous, $\gamma(1) = 1$.

Since the flux ratio is less than unity in the interior of the salt-finger interval but reaches unity at the endpoints, we have an important conclusion that $\gamma(R)$ has a minimum in the interior. It is interesting to note that existence of this minimum is reflected even in the Schmitt (1979*b*) fastest-growing finger model, although his theoretical $\gamma(R)$ curve does not reach unity at $R = 1$ but follows the pattern shown schematically in figure 2. While Schmitt's theory cannot be rigorously justified in the fully nonlinear regime ($R \ll 1/\tau$), laboratory experiments demonstrate that it performs surprisingly well (Kunze 2003) over a wide range of R. For the heat/salt fingers ($\tau = 0.01$ and $Pr = 7$), the fastest-growing finger model predicts $R_{min} = 4$, whereas for the sugar/salt solute ($\tau = 1/3$, $Pr = 10^3$), often used in the laboratory experiments (e.g. Krishnamurti 2003), $R_{min} = 1.3$.

The situation is somewhat different in the oceanic case, where the T, S fluxes are produced by a combination of double-diffusion and wave-generated turbulence. It is now commonly accepted (e.g. Kunze 2003) that fluxes in the ocean are controlled by turbulence for $R > 2$, whereas salt fingering dominates for sufficiently low R. Turbulence is characterized by nearly equal eddy diffusivities of heat and salt or, possibly, slightly higher diffusivity of heat if conditions favour differential diffusion (Gargett 2003). Thus, the flux ratio ($\gamma(R) = (K_T/K_S)R \approx R$) increases with R for $R > 2$ but decreases for smaller R, implying that the minimum of $\gamma(R)$ is below $R = 2$. Oceanographic observations show that staircases are confined to the regions where $R \lesssim 1.7$ (Schmitt 2003), suggesting that in the ocean $R_{min} \approx 1.7$ or slightly above.

To test the sensitivity of our theory (§ 3) to the assumed pattern of the $\gamma(R)$ relation, in table 1 we list the values of the equilibrium layer thickness from (18) for various R_{min} and $\bar{R}$. While the model predictions in the first two columns ($R_{min} = 1.7$ and $R_{min} = 2$) are consistent with observations, the values of $H_{0\,dim}$ for $R_{min} = 2.5$ (third column

in table 1) are unrealistically high, which supports our conjecture that, for typical oceanic conditions, the minimum of the flux ratio lies in the range $1.7 < R_{min} < 2$.

REFERENCES

Balmforth, N. J., Llewellyn Smith, S. G. & Young, W. R. 1998 Dynamics of interfaces and layers in a stratified turbulent fluid. *J. Fluid Mech.* **355**, 329–358.

Emanuel, K. 1994 *Atmospheric Convection*. Oxford University Press.

Gargett, A. E. 2003 Differential diffusion: an oceanographic primer. *Prog. Oceanogr.* **56**, 559–570.

Griffiths, R. W. & Ruddick, B. R. 1980 Accurate fluxes across a salt-sugar finger interface deduced from direct density measurements. *J. Fluid Mech.* **99**, 85–95.

Grossmann, S. & Lohse, D. 2000 Scaling in thermal convection: a unified theory. *J. Fluid. Mech.* **407**, 27–56.

Huppert, H. E. 1971 On the stability of a series of double-diffusive layers. *Deep-Sea Res.* **18**, 1005–1021.

Kelley, D. E., Fernando, H. J. S., Gargett, A. E., Tanny, J. & Ozsoy, E. 2003 The diffusive regime of double-diffusive convection. *Prog. Oceanogr.* **56**, 461–481.

Krishnamurti, R. 1995 Low-frequency oscillations in turbulent Rayleigh-Benard convection: laboratory experiments. *Fluid Dyn. Res.* **16**, 87–108.

Krishnamurti, R. 2003 Double-diffusive transport in laboratory thermohaline staircases. *J. Fluid Mech.* **483**, 287–314.

Kunze, E. 2003 A review of salt fingering theory. *Prog. Oceanogr.* **56**, 399–417.

Ledwell, J., Watson, A. & Law, C. 1993 Evidence for slow mixing across the pycnocline from an open-ocean tracer-release experiment. *Nature* **367**, 701–703.

Marmorino, G. O., Brown, W. K. & Morris, W. D. 1987 Two-dimensional temperature structure in the C-SALT thermohaline staircase. *Deep-Sea Res.* **23**, 1667–1675.

McDougall, T. J. 1991 Interfacial advection in the thermohaline staircase east of Barbados. *Deep-Sea Res.* **38**, 357–370.

Merryfield, W. J. 2000 Origin of thermohaline staircases. *J. Phys. Oceanogr.* **30**, 1046–1068.

Ozgokmen, T. M., Esenkov, O. E. & Olson, D. B. 1998 A numerical study of layer formation due to fingers in double-diffusive convection in a vertically-bounded domain. *J. Mar. Res.* **56**, 463–487.

Paparella, F. 2000 Fingering convection: the interplay of small and large scales. *Ann. NY Acad. Sci.* **898**, 144–158.

Radko, T. & Stern, M. E. 1999 Salt fingers in three dimensions. *J. Mar. Res.* **57**, 471–502.

Radko, T. & Stern, M. E. 2000 Finite-amplitude salt fingers in a vertically bounded layer. *J. Fluid Mech.* **425**, 133–160.

Radko, T. 2003 A mechanism for layer formation in a double-diffusive fluid. *J. Fluid Mech.* **497**, 365–380 (referred to herein as R03).

St. Laurent, L. & Schmitt, R. W. 1999 The contribution of salt fingers to vertical mixing in the North Atlantic tracer release experiment. *J. Phys. Oceanogr.* **29**, 1404–1424.

Schmitt, R. W. 1979*a* Flux measurements on salt fingers at an interface *J. Mar. Res.* **37**, 419–436.

Schmitt, R. W. 1979*b* The growth rate of super-critical salt fingers. *Deep-Sea Res.* **26A**, 23–40.

Schmitt, R. W. 1981 Form of the temperature-salinity relationship in the Central Water: evidence for double-diffusive mixing. *J. Phys. Oceanogr.* **11**, 1015–1026.

Schmitt, R. W., Perkins, H., Boyd, J. D. & Stalcup, M. C. 1987 C-SALT: an investigation of the thermohaline staircase in the western tropical North Atlantic. *Deep-Sea Res.* **34**, 1655–1665.

Schmitt, R. W. 1994 Double diffusion in oceanography. *Annu. Rev. Fluid Mech.* **26**, 255–285.

Schmitt, R. W. 2003 Observational and laboratory insights into salt finger convection. *Prog. Oceanogr.* **56**, 419–433.

Schmitt, R. W, Ledwell, J., Montgomery, E. T., Polzin, K. & Toole, J. 2004 Enhanced diapycnal mixing by salt fingers in the main thermocline of the tropical Atlantic. *Science* (submitted).

Stern, M. E. 1969 Collective instability of salt fingers. *J. Fluid Mech.* **35**, 209–218.

Stern, M. E. & Radko, T. 1998 The salt finger amplitude in unbounded T-S gradient layers. *J. Mar. Res.* **56**, 157–196.

Stern, M. E., Radko, T. & Simeonov, J. 2001 3D salt fingers in an unbounded thermocline with application to the Central Ocean. *J. Mar. Res.* **59**, 355–390.

Turner, J. S. 1967 Salt fingers across a density interface. *Deep-Sea Res.* **14**, 499–611.

Walsh, D. & Ruddick, B. R. 2000 Double-diffusive interleaving in the presence of turbulence: the effect of a nonconstant flux ratio. *J. Phys. Oceanogr.* **30**, 2231–2245.

Zodiatis, G. & Gasparini, G. P. 1996 Thermohaline staircase formations in the Tyrrhenian Sea. *Deep-Sea Res.* **43**, 665–678.